Received: 15 November 2018 | Accepted: 7 December 2018

DOI: 10.1002/jcp.28156

ORIGINAL RESEARCH ARTICLE

WILEY Journal of Cellular Physiology

Circular RNA hsa_circ_0007059 indicates prognosis and influences malignant behavior via AKT/mTOR in oral squamous cell carcinoma

Wen Su[1,2] | Yufan Wang[1] | Feng Wang[1] | Biru Zhang[1] | Hanyu Zhang[1] | Yuehong Shen[1] | Hongyu Yang[1]

[1]Department of Oral and Maxillofacial Surgery, Peking University Shenzhen Hospital, Shenzhen, Guangdong, China

[2]Clinical College, Peking University Shenzhen Hospital, Anhui Medical University, Shenzhen, Guangdong, China

Correspondence
Yuehong Shen and Hongyu Yang, Department of Oral and Maxillofacial Surgery, Peking University Shenzhen Hospital, No. 1120 Lianhua Road, Shenzhen, Guangdong 518036, China.
Email: yuehongshen@hotmail.com; hyyang192@hotmail.com

Funding information
National Natural Science Foundation of China, Grant/Award Number: 81572654; Basic Research Program of Shenzhen Innovation Council of China, Grant/Award Numbers: JCYJ20160428173933559, JCYJ20150403091443303, SZBC2017023, JCYJ20150403091443286; The Sanming Project for Medicine in Shenzhen, Grant/Award Numbers: Oral and Maxillofacial Surgery Tea, SZSM 201512036

Abstract

Oral squamous cell carcinoma (OSCC), the most common oral cancer, damages oral epithelial cells after the accumulation of multiple genetic mutations. Although emerging evidence supports the key role of circular RNAs (circRNAs) in various malignancies, the clinical value and function of circRNAs in OSCC remain unclear. In this study, patients with OSCC (n = 8) and controls (n = 8) were compared using high-throughput sequencing and microarray circRNA expression profiles. The circRNA hsa_circ_0007059 was downregulated in OSCC. Subsequently, hsa_circ_0007059 levels in OSCC tissues and cell lines were assessed by quantitative reverse-transcription chain reaction. Loss-of-function and gain-of-function experiments were performed to determine whether hsa_circ_0007059 affects malignant behavior in SCC15 and CAL27 cells. Importantly, hsa_circ_0007059 upregulation suppressed cell growth, migration, and invasion, facilitating apoptosis of these cells. Furthermore, nude mouse tumor formation was assessed to validate the tumor-suppressive role of hsa_circ_0007059 in vivo. Finally, hsa_circ_0007059 was determined to alter cell growth via AKT/mTOR signaling, representing a potential prognostic/therapeutic target for OSCC.

KEYWORDS
closed circular RNA, mouth neoplasms, mTOR protein, protein kinase B, squamous cell carcinoma

1 | INTRODUCTION

Head and neck squamous cell carcinoma (HNSCC) is the sixth most common cancer in the world (Siegel, Miller, & Jemal, 2016; Van Dijk, Brands, Geurts, Merkx, & Roodenburg, 2016). Oral squamous cell carcinoma (OSCC) is the most common malignancy and represents more than 90% of all head and neck cancers (Calcaterra & Juillard, 1995). The disease is responsible for more than 65,000 annual deaths in Europe alone (Thompson L, 2006). More than 50% of patients diagnosed with HNSCC suffer from local relapses, whereas up to 25% develop distant metastases. The prognosis for these patients remains poor (Haddad & Shin, 2008; Parkin, Bray, Ferlay, & Pisani, 2001; Zbaren & Lehmann, 1987).

Circular RNAs (circRNAs) are a newly discovered type of noncoding RNA ubiquitous to many species (Conn et al., 2015; Greene et al., 2017). Unlike canonical linear RNAs, circRNAs form a covalently closed continuous loop structure with neither 5′ caps nor 3′ polyadenylated tails, which makes them more stable than linear RNAs (Suzuki & Tsukahara, 2014). CircRNAs are abundant, diverse, stable, conserved, and characterized by localization and expression specificity (Jeck et al., 2013; Panda et al., 2017; Salzman, Gawad, Wang, Lacayo, & Brown, 2012). They have been

documented to act as a microRNA sponge (Hansen et al., 2013; Memczak et al., 2013) and participate in RNA polymerase II elongation (Li et al., 2015) and alternate splicing (Ashwal-Fluss et al., 2014).

High-throughput sequencing technology has revealed the key role of numerous circRNAs in human cancer (Bachmayr-Heyda et al., 2015; Dragomir & Calin, 2018). Because circRNA diversity varies with the type of tumor and degree of malignancy, some circRNAs have been shown to promote the development of tumors, whereas others can inhibit tumor proliferation and growth. Therefore, circRNAs represent a potential therapeutic target as well as a therapeutic vector (Cui et al., 2018; Patop & Kadener, 2018; Xu et al., 2018).

The present study analyzed the differential expression of hsa_circ_0007059 in OSCC specimens and adjacent nontumor tissues. Understanding the clinical relevance of hsa_circ_0007059 in OSCC may lead to the development of alternative treatment options for this common cancer.

2 | MATERIALS AND METHODS

2.1 | Patients and tissue samples

Oral cancer tissues and adjacent normal tissues were obtained from 52 patients with oral cancer at the Department of Oral and Maxillofacial Surgery, Peking University Shenzhen Hospital (Shenzhen, China), between 2016 and 2018. None of the patients had received chemotherapy or radiotherapy before the surgery. Tissue specimens were snap-frozen in liquid nitrogen immediately after resection and stored at −80°C until RNA extraction. Oral cancer was diagnosed and classified through pathological examination on the basis of the World Health Organization classification system (Thompson L, 2016).

Eight OSCC and normal tissue samples were sent for high-throughput sequencing (Guangzhou Gene Denovo Biotechnology Co. Ltd., Guangzhou, China). All patients gave their informed consent in accordance with the ethical guidelines of Peking University (Protocol No. 37923/2–3-2012). The study was approved by the Ethics Committee of Peking University Health Science Center (IRB00001053–08043).

2.2 | Cell culture and transfection

Human OSCC cell lines SCC9, SCC15, SCC25, and CAL27 were obtained from the College of Stomatology, Wuhan University (Wuhan, China). Human oral keratinocyte (HOK) cells were obtained from the cell bank of the Chinese Academy of Sciences (Shanghai, China). SCC15, SCC25, CAL27, and HOK cells were cultured in Dulbecco's modified Eagle's medium (DMEM; Gibco, Grand Island, NY) containing 10% fetal bovine serum (FBS; Gibco) and 1% penicillin/streptomycin (P/S; Life Technologies Inc., Carlsbad, CA). SCC9 cells were cultured in 1:1 DMEM/Ham's F12 medium containing 10% FBS and 1% P/S. All cells were cultured at 37°C and 5% CO_2 in a humidified atmosphere. To knock down hsa_circ_0007059, the cells were Infected with Lipofectamine 3000 (Gibco) and hsa_circ_0007059 siRNA (5′-CATCCAGCCAGGGACTGTT-3′) synthesized by Guangzhou RiboBio Co. (Guangzhou, China).

2.3 | Lentivirus infection and cell screening

The lentiviral vector was constructed at HanBio Co. Ltd. (Shanghai, China). The cells were plated in 24-well plates and cultured overnight at 37°C. After that, they were cultured for 48 hr in a complete medium containing the lentiviral vector. Monoclonal cell lines were selected using a complete medium containing puromycin(8 μg/mL for SCC15 cells; 10 μg/mL for CAL27 cells) and verified by quantitative reverse-transcription chain reaction (qRT-PCR) (Qcbio Science & Technologies Co. Ltd., Shanghai, China). After infection, green fluorescent protein (GFP) expression efficiency was observed by fluorescence microscopy.

2.4 | RNA preparation, treatment with RNase R, and qRT-PCR

Total RNA was isolated with an RNeasy Mini Kit (Qiagen, Hilden, Germany) according to the manufacturer's instructions. RNase R treatment was carried out for 15 min at 37°C using RNase R (Epicentre, Madison, WI) at 3 U/mg. Treated RNA (500 ng) was directly reverse-transcribed using the PrimeScript RT Master Mix (Takara Bio Inc., Kusatsu, Japan) with random or oligo(dT) primers. PCR was performed using 2 × PCR Master Mix (Thermo Fisher Scientific, Waltham, MA). The $\Delta\Delta^{Ct}$ method was used to calculate the relative expression of different genes, and glyceraldehyde 3-phosphate dehydrogenase (*GAPDH*) was used as an internal control. Primers for qRT-PCR were as follows: hsa_circ_0007059-F, 5′-GAGACAGTAGCCATCCAGC-3′; hsa_circ_0007059-R, 5′-TGATCTGAGTCCAGGTGTT-3′; GAPDH-F, 5′-TCAAGGCTGAGAACGGGAAG-3′; GAPDH-R, 5′-TCGCCCCACTTGATTTTGGA-3′.

2.5 | Cell Counting Kit-8 assay

Infected OSCC cells were plated into 96-well plates at 2×10^3 cells/well. At 0, 24, 48, 72, and 96 hr, 10 μl of the Cell Counting Kit-8 (CCK-8; Biyuntian Biotechnology Co. Ltd., Shanghai, China) and 90 μl of fresh medium were added to each well. The 96-well plate was then cultured for 1 hr. A microplate reader was used to measure the optical density (OD) at 450 nm and 630 nm. GraphPad 5.0 (GraphPad Software, La Jolla, CA) was used to analyze OD values and create a line plot.

2.6 | 5-ethynyl-2′-deoxyuridine incorporation assay

Logarithmically growing cells were seeded into 96-well plates at 4×10^3 cells/well and then cultured to 90% confluence. The cells were incubated for 2 hr with a diluted 5-ethynyl-2′-deoxyuridine

(EdU) solution, fixed with 4% paraformaldehyde in phosphate-buffered saline (PBS; Beyotime Biotechnology, Shanghai, China), and incubated for 30 min at room temperature. Afterward, Apollo and Hoechst 33342 (Beyotime Biotechnology) reaction solutions were used to stain the cells under room temperature conditions, respectively. The cells were photographed using an inverted fluorescence microscope, counted by ImageJ (NIH, Bethesda, MD), and statistically analyzed with GraphPad 5.0.

2.7 | Flow cytometry

The cells were routinely infected, cultured for 48 hr, and then digested with trypsin. An Annexin V-FITC/propidium iodide (PI) Apoptosis Assay Kit (Biyuntian Biotechnology Co. Ltd.) was used to estimate the apoptotic rate according to the manufacturer's instructions. The cells were suspended in 1 × Annexin V-binding buffer, and then 5 μl of Annexin V and 1 μl of PI were added to 100 μl of cell suspension and mixed. The mixture was incubated in the dark for 15 min at room temperature, after which 400 μl of the 1 × Annexin V-binding buffer was added to each sample to terminate the reaction. The rate of apoptosis was determined using a FACSCalibur flow cytometer (BD Biosciences, Franklin Lakes, NJ).

2.8 | Hoechst 33258 staining

Initially, 4×10^5 cells/well were placed into a 24-well plate containing sterilized slides and incubated overnight. The cells were fixed in 4% paraformaldehyde for 15 min. Hoechst 33258 staining solution (Biyuntian Biotechnology Co. Ltd.) was added under the darkness and incubated for 10–15 min. One drop of anti-fluorescence quenching mounting solution was placed on each slide. After air-drying at room temperature, an inverted fluorescence microscope was used to observe the samples at 350 nm/460 nm excitation/emission wavelengths. Nuclear morphology and typical apoptotic changes (chromatin condensation, agglutination, and disruption) were recorded.

2.9 | Wound healing assay

Infected cells were spread on six-well plates and cultured until confluent. Before wounding, the cells were cultured in DMEM without FBS for 1 day. A sterile 200-μl pipette tip was used to scratch the cell monolayers. After wounding, the cells were washed three times with PBS and incubated with fresh medium without FBS. Images were acquired at 0 and 24 hr.

2.10 | Migration and invasion assays

Migration and invasion assays were performed using Transwell and Matrigel pre-coated Transwell chambers, respectively (Corning Life Sciences, Corning, NY). The cells were resuspended in DMEM without FBS and added to the upper chamber, whereas the medium containing 10% FBS was added to the lower chamber. After incubation for 24 or 48 hr, the cells in the upper chamber were removed, and those in the lower chamber were fixed in 4% paraformaldehyde, stained with 0.1% crystal violet, washed with PBS, and dried. The images were acquired using an inverted fluorescence microscope and processed using ImageJ, and the data were analyzed by SPSS 17.0 software (IBM, Chicago, IL).

2.11 | Inhibitor experiment

The untreated tumor cells were cultured for 24 hr (IC50: SCC15: 13.97 uM; CAL27: 5.46 uM) in a medium containing MK-2206 2HCl (Selleck, Shanghai, China), then the virus or siRNA was added and the incubation continued for 48 hr, the proteins were extracted for subsequent experiments.

2.12 | Western blot analysis

Cell and nude mouse tumor tissues extracts were prepared at 4°C in RIPA buffer (Beyotime Biotechnology). The western blot analysis was performed using commercial primary antibodies against the following proteins: Bcl-2 (1:2,000; ab32124), Bax (1:2,000; ab32503), MMP-9 (1:2,000; ab38898), cyclin D1 (1:2,000; ab134175), GAPDH (1:2,000; ab8245, all from Abcam, Cambridge, UK), vimentin (1:1,000; #5741 T), AKT (1:1,000; #4691), p-AKT (1:2,000; #4060), mTOR (1:1,000; #2983), and p-mTOR (1:1,000; #5536, all from Cell Signaling Technology, Danvers, MA).

Immunoreactive bands were detected using horseradish peroxidase-conjugated goat antirabbit (1:1,000; A0208) and goat anti-mouse (1:1,000; A0216, both from Beyotime Biotechnology) secondary antibodies. Chemiluminescence was detected using the Millipore chromogenic solution (Millipore Sigma, Burlington, MA).

2.13 | Tumorigenesis and staining

Infected SCC15 cells (1×10^7 cells/100 μl) were injected into 16 4-week-old BALB/c athymic nude mice (Silaike Jingda Experimental Animal Co. Ltd., Hunan, China). Tumor volume, measured weekly, was calculated as $V = \pi AB^2/6$, where V = tumor volume, A = largest diameter, and B = perpendicular diameter. After 6 weeks, the nude mice were euthanized and weighed. Animal experiments were undertaken with the approval of the Institutional Committee for Animal Research and in conformity with the national guidelines for the care and use of laboratory animals.

2.14 | Image processing and statistical analysis

All images are wide-field microscopy images. Results in graphs represent the mean ± standard error of the mean (SEM) from three independent experiments. All statistical data were analyzed using SPSS 17.0 software. Two-tailed Student's *t* tests were used to determine *p* values; $p < 0.05$ was considered significant.

3 | RESULTS

3.1 | Hsa_circ_0007059 is lowly expressed in OSCC

In our experiments, high-throughput sequencing was used to acquire microarray circRNA expression profiles from patients with OSCCs ($n = 8$) and controls ($n = 8$). The circRNA expression profiles revealed significantly lower hsa_circ_0007059 mRNA levels in OSCC compared with adjacent tissues (Wang et al., 2018). Here, we found that the circRNA hsa_circ_0007059 is abnormally expressed in OSCC. The parent gene of hsa_circ_0007059 is *ZNF720*; its position on the chromosome is chr16: 31733946–31734674. Subsequently, 52 pairs of clinical OSCC tissues and adjacent normal tissues were analyzed by qRT-PCR. The expression level of hsa_circ_0007059 was lower in OSCC compared with the control tissue (Figure 1a). The clinicopathological parameters of the 52 patients with OSCC are shown in Table 1. In addition, we investigated the expression level of hsa_circ_0007059 in four OSCC cell lines: SCC15, SCC25, SCC9, and CAL27. Compared with that in the HOK normal oral keratinocyte cell line, expression of hsa_circ_0007059 was lower in OSCC cells (Figure 1b).

3.2 | Elevated expression of hsa_circ_0007059 reduces proliferation and promotes apoptosis in OSCC cells

Lentivirus particles containing hsa_circ_0007059 were stably infected into SCC15 and CAL27 cells. Puromycin and fluorescent microscopy were then used to screen for stable strains emitting green fluorescence. Expression efficiency was about 94.8- and 70.8-fold, respectively (Figure 1c,d). qRT-PCR quantification of hsa_circ_0007059 levels in SCC15 and CAL27 cells transfected with hsa_circ_0007059 siRNA are shown in Figure 1e and Figure 1f.

To investigate the role of hsa_circ_0007059 in regulating cell proliferation, we performed the CCK-8 assay in SCC15 and CAL27 cells. OD values were recorded at 450 nm and 630 nm at different time points. As the incubation time increased, the proliferation rate

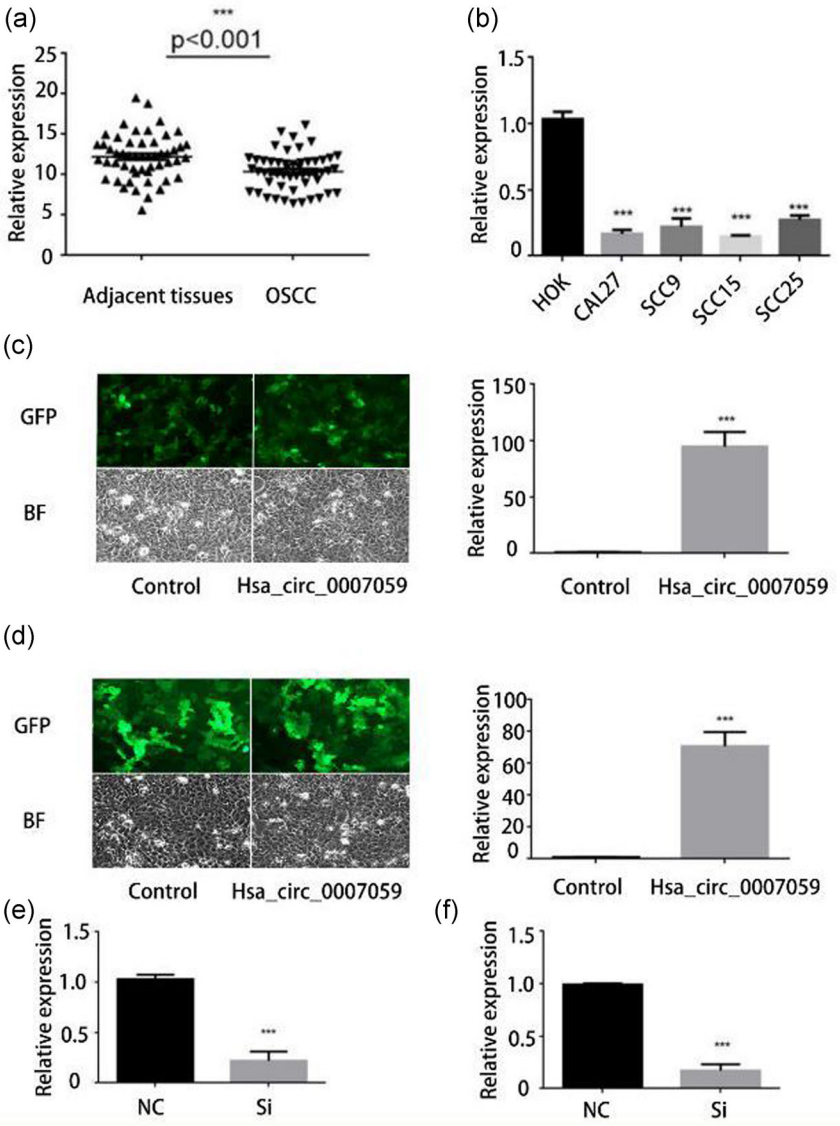

FIGURE 1 Hsa_circ_0007059 is downregulated in OSCC tissue specimens and cell lines. (a,b) qRT-PCR was used to determine the hsa_circ_0007059 expression level in (a) tumor tissue specimens from patients with OSCC, relative to that in adjacent normal tissues ($n = 52$); and (b) HOK, CAL27, SCC9, SCC15, and SCC25 cell lines. (c,d) The hsa_circ_0007059 expression level in stable SCC15 (c) and CAL27 (d) cell lines was quantified using qRT-PCR. GFP expression was examined under a fluorescence microscope in stable SCC15 and CAL27 cell lines. BF refers to the bright field. (e,f) qRT-PCR quantification of hsa_circ_0007059 levels in SCC15 (e) and CAL27 (f) cells transfected with hsa_circ_0007059 siRNA. Si and NC refer to OSCC cells transfected with hsa_circ_0007059 siRNA or normal control. The data are presented as means ± SEM of three independent experiments. Student's *t* test, $^{***}p < 0.001$. GFP: green fluorescent protein; OSCC: oral squamous cell carcinoma; qRT-PCR: quantitative reverse-transcription chain reaction; SEM: standard error of mean; siRNA: small interfering RNA [Color figure can be viewed at wileyonlinelibrary.com]

TABLE 1 Correlation between hsa_circ_0007059 expression and clinicopathological characteristics in 52 patients with oral squamous cell carcinoma

Items	Total cases (n = 52)	p value
Gender		
Male	40	0.88
Female	12	
Age (years)		
< 60	33	0.82
≥ 60	19	
Clinical stage		
I + II	21	0.11
III + IV	31	
Pathological differentiation		
Well	20	0.33
Moderately	18	
Poorly	14	
Lymph node metastasis		
Yes	22	0.041*
No	30	

of the cells in the test group decreased significantly compared with that of the control group (Figure 2a,b). Proliferation results were confirmed by EdU staining, whereas the nuclei of cells in the S phase were stained red. Elevated expression of hsa_circ_0007059 caused the proliferation ratio to decrease by about 17% and 12.3% in SCC15 and CAL27 cells, respectively, compared with that of the control group (Figure 2c,d).

Annexin V-FITC/PI dual-label flow cytometry was performed to determine the rate of apoptosis in OSCC cells. For SCC15 cells, the proportion of cells in early apoptosis was 14.46%, a value substantially higher than that of the control group (1.24%; Figure 3a). Similarly, the proportion of CAL27 cells in early apoptosis was 13.78% in the test group and only 0.06% in the control group (Figure 3b). These results indicated that the elevated expression of hsa_circ_0007059 significantly promotes apoptosis in SCC15 and CAL27 cells. Moreover, SCC15 and CAL27 cells infected with lentivirus were stained by Hoechst, and the number of apoptotic cells in each group was counted, revealing 4.5-fold (SCC15) and 4.3-fold (CAL27) more apoptotic cells in the test group than in the control group (Figure 3c). Taken together, these findings suggested that the elevated expression of hsa_circ_0007059 reduces OSCC cell proliferation and promotes cell apoptosis.

3.3 | Elevated expression of hsa_circ_0007059 inhibits the migration and invasion ability of OSCC cells

To determine the function of hsa_circ_0007059 in regulating OSCC cell migration, a wound healing assay was performed. The scratch area was measured at 0 and 24 hr after wounding. Notably, high expression of hsa_circ_0007059 significantly reduced the wound closure rate compared with that of control cells. The closure percentage at 24 hr was 52.97% (SCC15; Figure 4a) and 71.33% (CAL27; Figure 4b), which was substantially lower than 70.68% and 87.83%, respectively, observed in control cells. A Transwell migration assay was performed to study the migration ability of OSCC cells expressing high levels of hsa_circ_0007059. After 24 hr of incubation, the average number of cells passing through the chamber was 456.33 (SCC15) and 617.33 (CAL27) in the test groups, as opposed to 629.66 and 849.33, respectively, in the control groups (Figure 4c). Overall, the OSCC cell migration ability was reduced after the high expression of hsa_circ_0007059. To investigate the invasion ability of OSCC cells, we performed a Transwell invasion assay. After 48 hr of incubation, the number of cells that crossed the chamber coated with Matrigel was measured. Elevated expression of hsa_circ_0007059 significantly decreased the cell invasion ability. For both SCC15 and CAL27, the number of invading cells in the test group was only around 50% that of the control group (Figure 4d). Taken together, these results suggested that hsa_circ_0007059 regulates OSCC cell migration and invasion.

3.4 | Hsa_circ_0007059 regulates tumor growth through the AKT/mTOR signaling pathway

To investigate the molecular basis of the regulation of OSCC cells by hsa_circ_0007059, we measured the expression of several proteins by western blotting. High expression of hsa_circ_0007059 resulted in upregulation of Bax but downregulation of Bcl-2, MMP-9, and cyclin D1 (Figure 5a). The opposite result was obtained when siRNA was used to knock down the expression of hsa_circ_0007059 (Figure 5b).

Studies have shown that the AKT/mTOR signaling pathway was crucial for epithelial cancer metastasis (Bahmad et al., 2018; Ocana et al., 2014; Rehan & Bajouh, 2019). To investigate the role of the AKT/mTOR pathway in OSCC, we either overexpressed or knocked down hsa_circ_0007059 and then detected AKT and mTOR variants by western blotting. Changes in the expression level of hsa_circ_0007059 did not produce any significant variation in the levels of AKT and mTOR, but they altered the levels of the phosphorylated forms, p-AKT, and p-mTOR (Figure 5c,d). This result indicated that hsa_circ_0007059 may be involved in the regulation of the AKT/mTOR signaling pathway.

Due to the change of hsa_circ_0007059 content, both p-AKT and p-mTOR were changed. To explore whether hsa_circ_0007059 only affects p-AKT content and then changes p-mTOR or other pathways affect p-mTOR, we design experiments. After inhibition of AKT expression in SCC15 and CAL27 cells by the AKT inhibitor MK-2206 2HCl (Selleck), the expression level of p-mTOR was successively decreased. At this time, we used lentivirus to infect or transfect the cells with SiRNA, and found that the change of hsa_circ_0007059 content in the cells did not cause significant changes in p-mTOR (Figure 5e,f). The above experimental results indicate that hsa_circ_0007059 can only cause changes in the downstream target gene p-mTOR by affecting the change of AKT content.

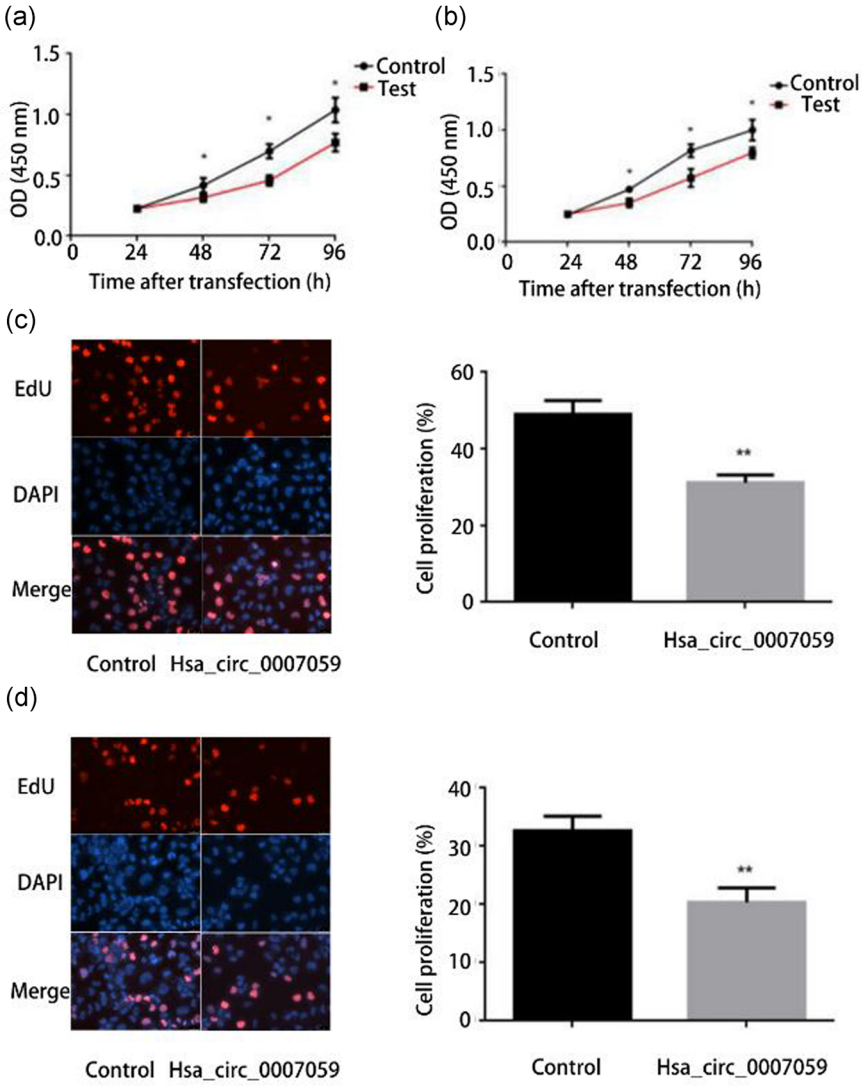

FIGURE 2 High expression of hsa_circ_0007059 inhibits OSCC cell proliferation. (a,b) SCC15 (a) and CAL27 (b) cells were infected with empty vector control (control) or lentivirus harboring hsa_circ_0007059 (test), and the CCK-8 assay was used to measure cell proliferation at different times after infection. (c,d) The EdU incorporation assay was used to measure the proliferation ratio in control SCC15 (c) and CAL27 (d) cells and those overexpressing hsa_circ_0007059. The data are presented as means ± SEM of three independent experiments. Student's *t* test, ***$p < 0.001$, **$p < 0.01$, *$p < 0.05$, Scale bar, 20 μm. CCK-8: cell counting kit-8; GFP: green fluorescent protein; OSCC: oral squamous cell carcinoma; SEM: standard error of mean [Color figure can be viewed at wileyonlinelibrary.com]

To investigate the potential of hsa_circ_0007059 as a new OSCC therapeutic target, we established a xenograft tumor model using the SCC15 cell line in nude mice. SCC15 cells were infected with lentivirus to induce high expression of hsa_circ_0007059. All mice developed tumors at the injection sites, but the tumors in the test group were much smaller compared with those in the empty vector group (Figure 6a). The tumor growth and final weight were recorded. Compared with those of the control group, the high expression of hsa_circ_0007059 decreased both the tumor growth rate and tumor weight in nude mice (Figure 6b,c). The AKT/mTOR signaling pathway markers in nude mouse tumor specimens were also detected by western blotting. The experimental results are consistent with the cytology experiments (Figure 6d). Taken together, these findings suggested that hsa_circ_0007059 is crucial for tumor growth and may potentially serve as a new therapeutic target for the OSCC treatment.

4 | DISCUSSION

Head and neck cancer encompasses cancers of the oral cavity, paranasal sinuses, pharynx, and larynx (Noguti et al., 2012; Vokes, Weichselbaum, Lippman, & Hong, 1993). Among all subtypes of oral malignancies, 90% belong to OSCC (Feller & Lemmer, 2012), which is a locally aggressive tumor whose invasion and ability to metastasize result from adaptation to the host microenvironment (Eckert, Kappler, Schubert, & Taubert, 2012). For this reason, the 5-year survival rate remains stubbornly high at 50–55%, in spite of aggressive treatment regimens encompassing radiation therapy, chemotherapy, and surgery (Heo et al., 2012). OSCC is characterized by genomic and epigenomic alterations. However, the mechanisms underlying OSCC tumorigenesis and progression remain to be elucidated. Therefore, to improve the survival rate of patients with OSCC, increasing research has focused on identifying effective therapeutic targets.

CircRNAs are newly discovered regulatory RNAs that possess low or no protein-coding potential. Emerging lines of evidence indicate that deregulated expression of circRNAs is associated with the induction and progression of various cancers, including oral cancer, through epigenetic, transcriptional, and posttranscriptional alterations (Balas & Johnson, 2018). In recent years, the role of circRNAs in tumorigenesis and development has attracted widespread attention, as the abnormal

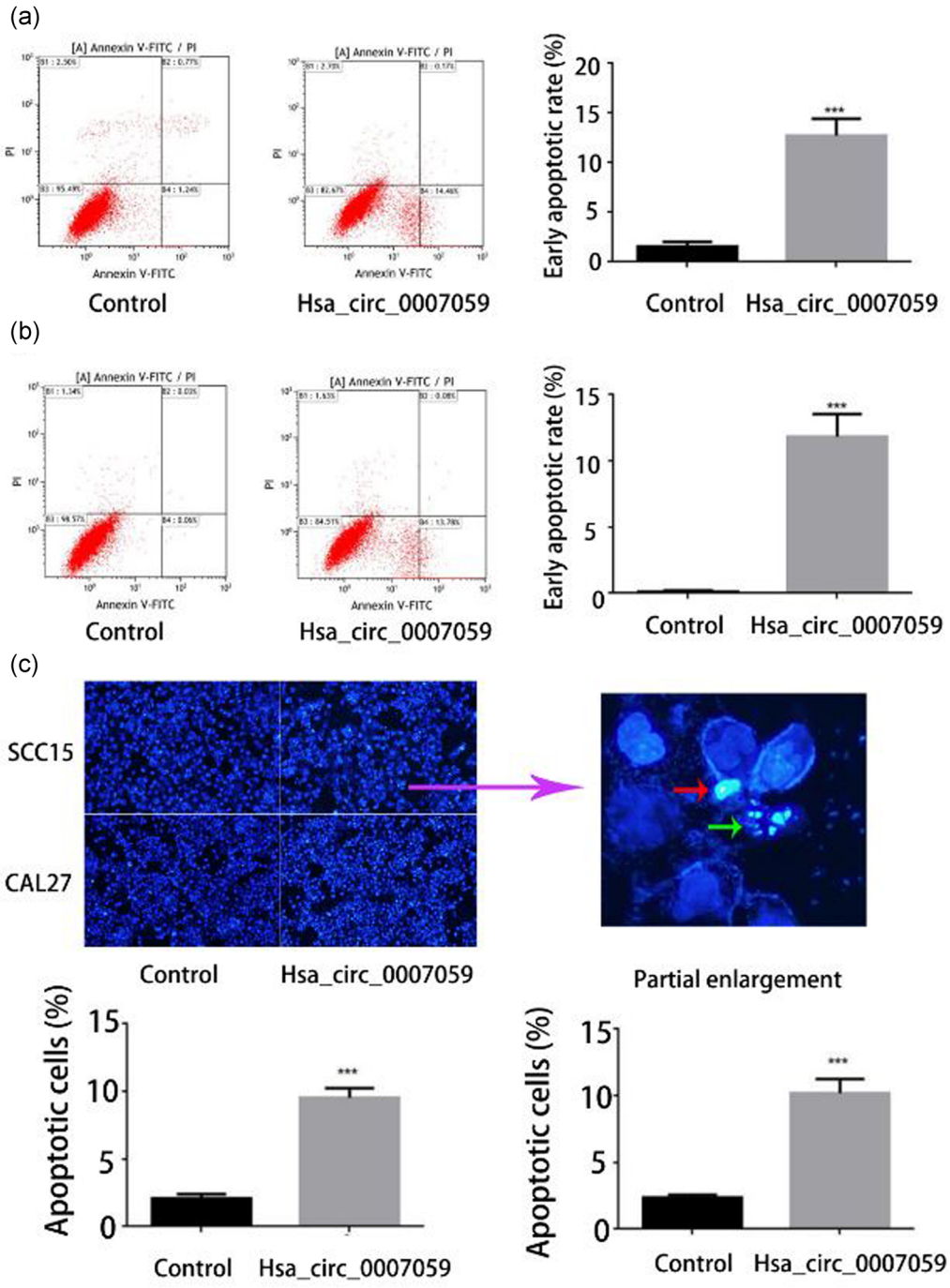

FIGURE 3 High expression of hsa_circ_0007059 promotes apoptosis in OSCC cells. (a,b) Annexin V-FITC/PI dual-label flow cytometry was performed to determine the apoptotic rate in SCC15 (a) and CAL27 (b) cells. (c) Hoechst staining was performed on SCC15 and CAL27 cells infected with empty vector control or lentivirus harboring hsa_circ_0007059. In a partial enlargement, the red arrow refers to the condensed nucleus, and the green arrow refers to the fragmented nucleus. The proportion of apoptotic cells was quantified in SCC15 (left) and CAL27 (right) cells. The data are presented as means ± SEM of three independent experiments. Student's *t* test, ***$p < 0.001$. OSCC: oral squamous cell carcinoma; SEM: standard error of mean [Color figure can be viewed at wileyonlinelibrary.com]

expression of circRNAs in various tumors has been reported (Greene et al., 2017; Kristensen, Hansen, Venø, & Kjems, 2018). However, research on the involvement of circRNAs in OSCC is still in its infancy.

To investigate the clinical value of hsa_circ_0007059 in OSCC, we collected 52 pairs of OSCC and adjacent tissue. The results showed that the level of hsa_circ_0007059 was lower in tumor tissue samples than in normal oral epithelial tissues. In addition, this downregulation was closely related to lymph node metastasis (Table 1). The above results indicated that downregulation of hsa_circ_0007059 may contribute to the progression of OSCC.

Given the downregulation of hsa_circ_0007059 in OSCC tissues, we sought to determine whether it affected the behavior of OSCC

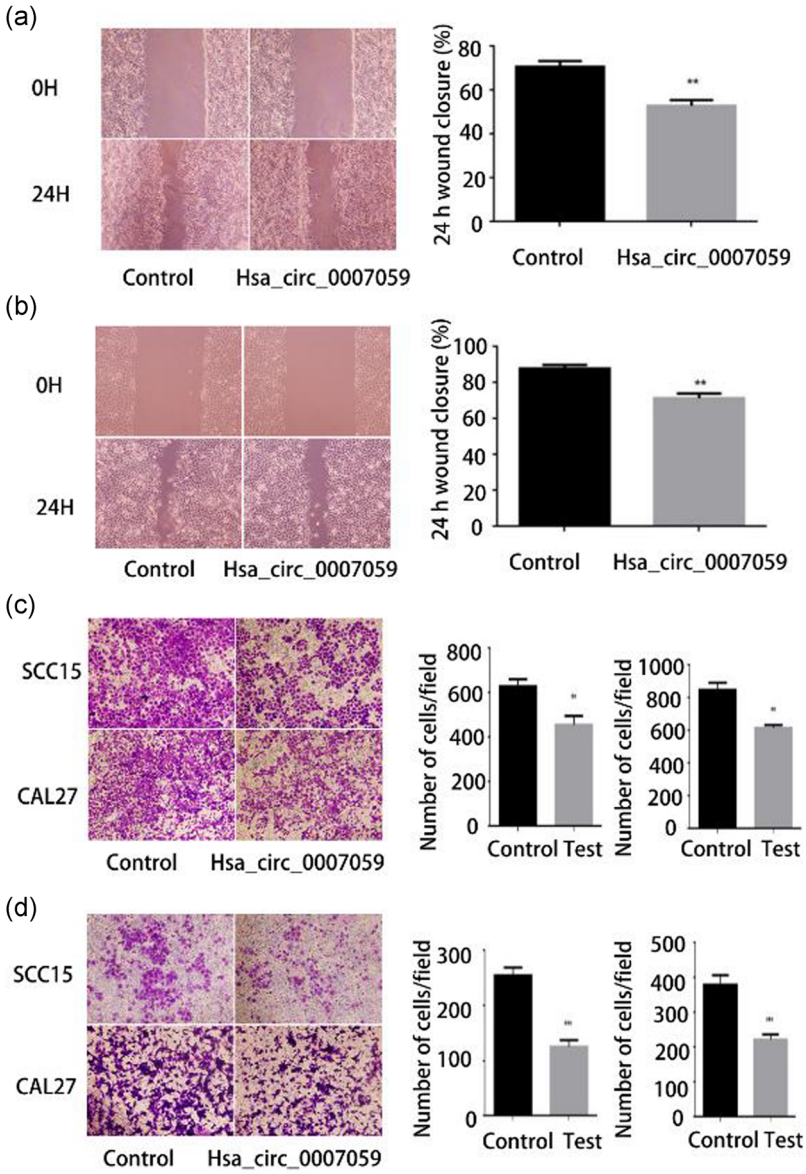

FIGURE 4 High expression of hsa_circ_0007059 inhibits OSCC cell migration and invasion. (a,b) Wound healing assays were performed on (a) SCC15 and (b) CAL27 cells infected with empty vector control or lentivirus harboring hsa_circ_0007059. The scratch area was measured at 0 and 24 hr, and the percentage of closure at 24 hr was calculated. (c,d) Transwell assays were performed to quantify the migration and invasion ability of SCC15 and CAL27 cells infected with empty vector control or lentivirus harboring hsa_circ_0007059. (c) The cells were seeded into the upper chamber (uncoated); after 24 hr, those that crossed to the lower chamber were imaged and quantified: SCC15 (top), CAL27 (bottom). The proportion of migrating cells was quantified in SCC15 (left) and CAL27 (right) cells. (d) The cells were seeded into the Matrigel-coated upper chamber; after 48 hr, those that passed across the coated chamber were imaged and quantified: SCC15 (top), CAL27 (bottom). The proportion of invading cells was quantified in SCC15 (left) and CAL27 (right) cells. The data are presented as means ± SEM of three independent experiments. Student's *t* test, $^{***}p < 0.001$, $^{**}p < 0.01$. OSCC: oral squamous cell carcinoma; SEM: standard error of mean [Color figure can be viewed at wileyonlinelibrary.com]

cell lines. To this end, we investigated the effect of high hsa_circ_0007059 expression in vitro. As expected, high expression of hsa_circ_0007059 significantly inhibited the proliferation, migration, and invasion of SCC15 and CAL27 tumor cell lines and promoted apoptosis of these cells. Apoptosis is a form of programmed cell death triggered by various factors, and mitochondrial apoptosis has been shown to play a crucial role. Bcl-2 and Bax proteins regulate apoptosis through the mitochondrial pathway. Bax promotes apoptosis by enhancing mitochondrial permeability and promoting the release of cytochrome c, whereas Bcl-2 inhibits mitochondrial apoptosis by binding to Bax (Evan & Littlewood, 1998). Cyclin D1 is an important regulatory protein of the cell cycle (Jirawatnotai, Hu, Livingston, & Sicinski, 2012), and MMP-9 is closely related to tumor cell migration and invasion (Bates, Gomez Hernandez, Lanzel, Qian, & Brogden, 2018). We showed that the expression of these key proteins in SCC15 and CAL27 cells changed significantly after increasing or knocking down the expression of hsa_circ_0007059. In addition, we report that the high expression of hsa_circ_0007059 significantly inhibited the malignant behavior of OSCC cells. In contrast, low expression of hsa_circ_0007059 did not cause significant changes in the malignant behavior of the cells, even though it altered the corresponding protein level. We speculate that the expression of the circRNA in the OSCC cell lines was originally very low and this contributed to the high degree of malignancy.

AKT plays a key role in many signaling pathways that contribute to the different biological properties of tumors (Rivas, Gómez-Oro, Antón, & Wandosell, 2018). Therefore, to determine the molecular mechanism by which hsa_circ_0007059 affected the malignant behavior of OSCC cells, we examined the expression of proteins associated with the AKT/mTOR signaling pathway. Accordingly, hsa_circ_0007059 expression was negatively correlated with the expression of p-AKT and p-mTOR but had little effect on the levels of total AKT and mTOR. We extracted nude mouse tumor specimens and tested key indicators of the AKT/mToR pathway, and the results were consistent with cytology experiments. At the same time, we also designed experiments to prove that the change of p-mTOR is only due to the influence of

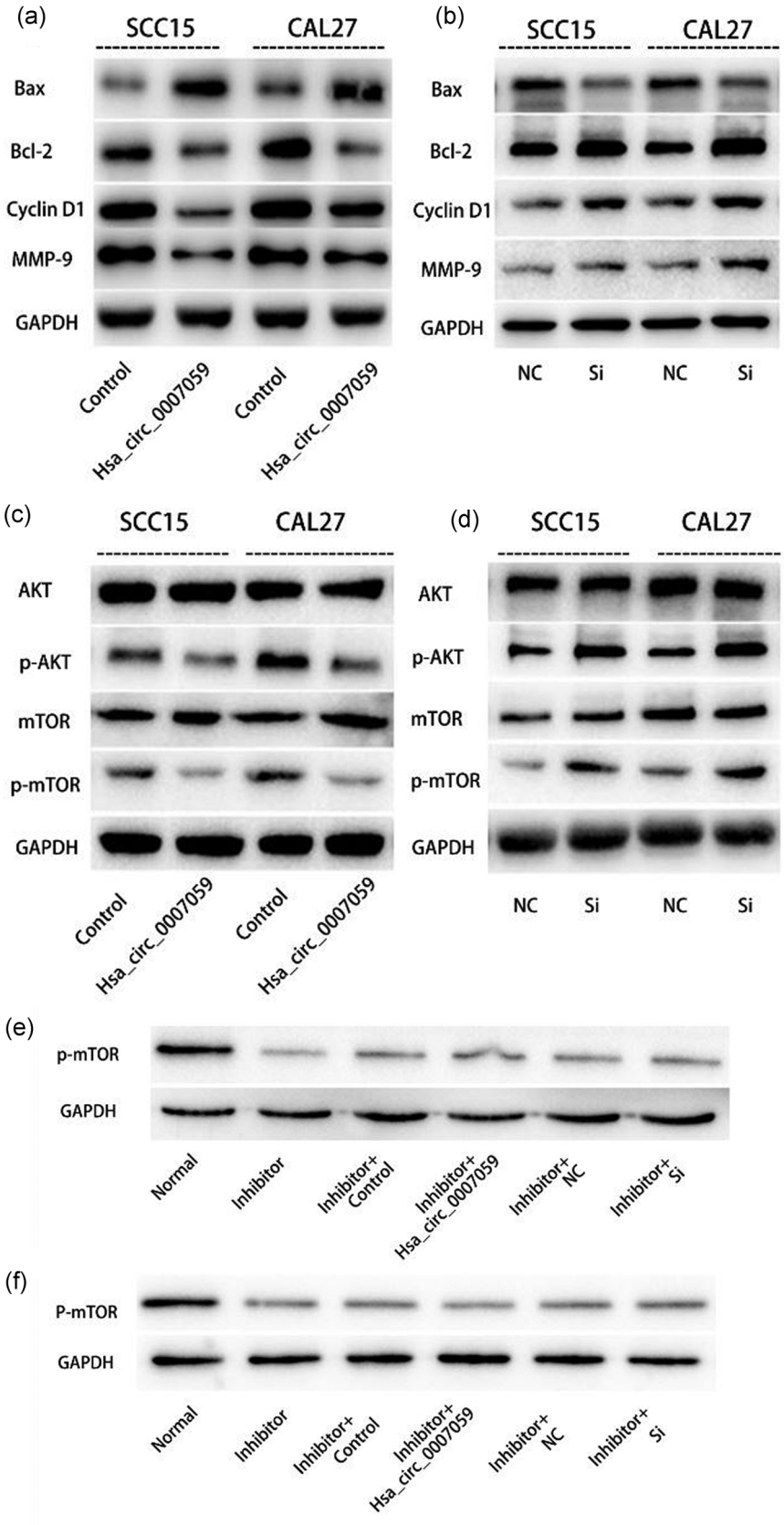

FIGURE 5 Expression of hsa_circ_0007059 affects the levels of key proteins involved in cell proliferation, apoptosis, invasion, and the AKT/mTOR signaling pathway. (a,b) SCC15 and CAL27 cells were subjected to either overexpression (left) or knockdown (right) of hsa_circ_0007059, cell extracts were immunoblotted, and the levels of key proteins related to proliferation, apoptosis, and invasion, such as Bax, Bcl-2, Cyclin D1, and MMP-9, were determined. (c,d) The AKT/mTOR signaling pathway markers were detected by western blotting. (e,f) The AKT/mTOR signaling pathway marker p-mTOR was detected by western blotting when using AKT inhibitors in SCC15 (e) and CAL27 (f) cells. GAPDH: glyceraldehyde 3-phosphate dehydrogenase

hsa_circ_0007059 on the expression of p-AKT rather than through other pathways. Overall, this finding indicates that downregulated hsa_circ_0007059 can promote OSCC cell growth by modulating the AKT/mTOR signaling pathway.

OSCC is a solid tumor characterized by multiple multi-step genetic alterations that lead to genomic instability and disordered cell growth due to oncogene overexpression, underexpression of tumor suppressor genes, and other genetic and epigenetic alterations (Abudayyeh et al.,

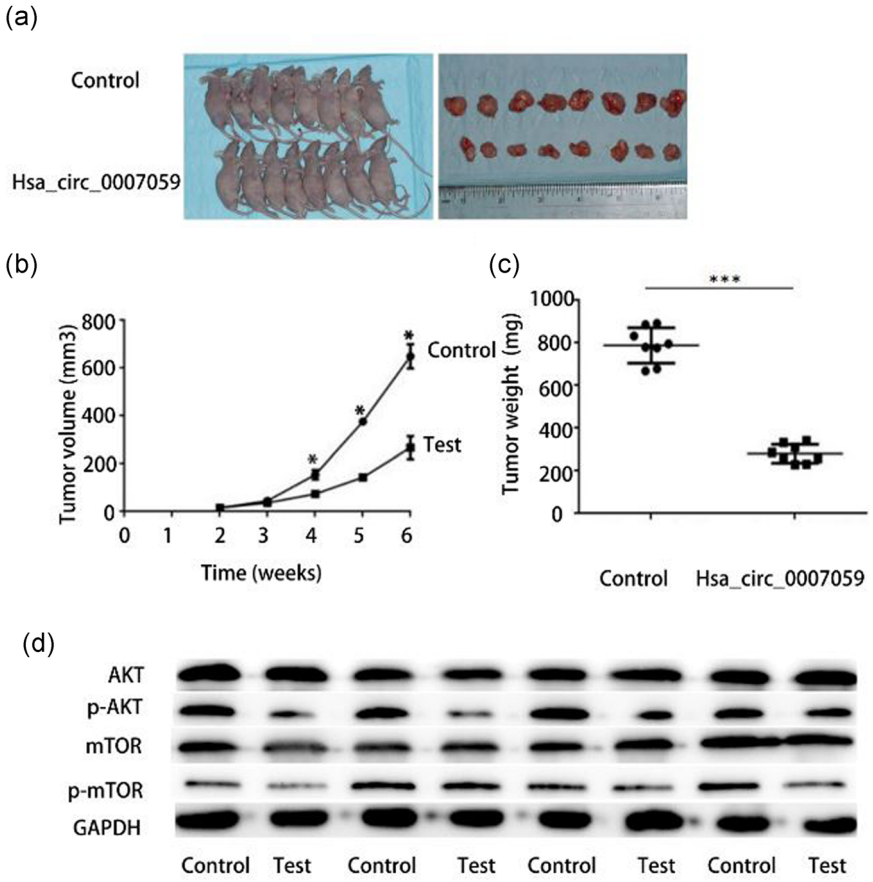

FIGURE 6 High expression of hsa_circ_0007059 inhibits tumorigenesis. (a) Pictures of nude mice bearing xenograft tumors generated using stable SCC15 cells and of surgically removed tumors. (b) Tumor growth curve showing a change in tumor volume in the weeks after injection. (c) Tumor weight plots of empty vector control (control) and hsa_circ_0007059 overexpression groups (test). (d) The AKT/mTOR signaling pathway markers in nude mouse tumor specimens were detected by western blotting. GAPDH: glyceraldehyde 3-phosphate dehydrogenase [Color figure can be viewed at wileyonlinelibrary.com]

2017; Aktaş et al., 2017; Armakola et al., 2012; Ashwal-Fluss et al., 2014). The sponge absorption function of circRNAs has been extensively studied and reported (Hansen et al., 2013; Memczak et al., 2013). We have predicted through bioinformatics software (https://circinteractome.nia.nih.gov) that the possible absorption targets of hsa_circ_0007059 include hsa-miR-593, hsa-miR-383, and hsa-miR-188-3p. However, elucidating the specific mechanism by which this interaction may play a role in OSCC will require further experiments.

In summary, this study reports the expression level and functional role of hsa_circ_0007059 in OSCC. Our results show that hsa_circ_0007059 is significantly reduced in OSCC tissues and cell lines compared with normal oral epithelial tissues and normal oral mucosal epithelial cells. Downregulation of hsa_circ_0007059 is associated with an invasive tumor phenotype, and thus hsa_circ_0007059 acts as a tumor suppressor in OSCC cells. Importantly, hsa_circ_0007059 regulates cell growth by modulating the AKT/mTOR signaling pathway. Our experimental results show that hsa_circ_0007059 may be a potential therapeutic target for OSCC.

ACKNOWLEDGMENTS

This study was supported by the National Natural Science Foundation of China (grant 81572654), the Basic Research Program of Shenzhen Innovation Council of China (grants JCYJ20150403091443303, JCYJ20150403091443286, JCYJ2016042873933559, and SZBC2017023), and the Sanming Project for Medicine in Shenzhen (SZSM 201512036, Oral and Maxillofacial Surgery Team, Professor Yu Guangyan, Stomatology Hospital Peking University). We sincerely thank Dr. Luo Weijia for providing encouragement.

CONFLICTS OF INTEREST

The authors declare that there are no conflicts of interest.

ORCID

Wen Su http://orcid.org/0000-0002-0278-9186
Yuehong Shen http://orcid.org/0000-0001-8080-7039
Hongyu Yang http://orcid.org/0000-0002-0367-4938

REFERENCES

Abudayyeh, O. O., Gootenberg, J. S., Essletzbichler, P., Han, S., Joung, J., Belanto, J. J., … Zhang, F. (2017). RNA targeting with CRISPR-Cas13. *Nature*, *550*(7675), 280–284.

Aktaş, T., Avşar Ilık, İ., Maticzka, D., Bhardwaj, V., Pessoa Rodrigues, C., Mittler, G., … Akhtar, A. (2017). DHX9 suppresses RNA processing defects originating from the Alu invasion of the human genome. *Nature*, *544*(7648), 115–119.

Armakola, M., Higgins, M. J., Figley, M. D., Barmada, S. J., Scarborough, E. A., Diaz, Z., … Gitler, A. D. (2012). Inhibition of RNA lariat debranching enzyme suppresses TDP-43 toxicity in ALS disease models. *Nature Genetics*, *44*(12), 1302–1309.

Ashwal-Fluss, R., Meyer, M., Pamudurti, N. R., Ivanov, A., Bartok, O., Hanan, M., … Kadener, S. (2014). circRNA biogenesis competes with pre-mRNA splicing. *Molecular Cell*, *56*, 55–66.

Bachmayr-Heyda, A., Reiner, A. T., Auer, K., Sukhbaatar, N., Aust, S., Bachleitner-Hofmann, T., … Pils, D. (2015). Correlation of circular RNA abundance with proliferation-exemplified with colorectal and ovarian cancer, idiopathic lung fibrosis, and normal human tissues. *Scientific Reports*, *5*, 8057.

Bahmad, H. F., Mouhieddine, T. H., Chalhoub, R. M., Assi, S., Araji, T., Chamaa, F., … Abou-Kheir, W. (2018). The Akt/mTOR pathway in cancer stem/progenitor cells is a potential therapeutic target for glioblastoma and neuroblastoma. *Oncotarget*, *9*(71), 33549–33561.

Balas, M. M., & Johnson, A. M. (2018). Exploring the mechanisms behind long noncoding RNAs and cancer. *Noncoding RNA Research*, *3*(3), 108–117.

Bates, A. M., Gomez Hernandez, M. P., Lanzel, E. A., Qian, F., & Brogden, K. A. (2018). Matrix metalloproteinase (MMP) and immunosuppressive biomarker profiles of seven head and neck squamous cell carcinoma (HNSCC) cell lines. *Translation Cancer Research*, *7*(3), 533–542.

Calcaterra, T. C., & Juillard, G. J. (1995). Oral cavity and hypopharynx-head and neck cancer, *Cancer treatment*. Philadelphia: WB Saunders Co. 726–732.

Conn, S. J., Pillman, K. A., Toubia, J., Conn, V. M., Salmanidis, M., Phillips, C. A., … Goodall, G. J. (2015). The RNA binding protein quaking regulates formation of circRNAs. *Cell*, *160*, 1125–1134.

Cui, X., Wang, J., Guo, Z., Li, M., Li, M., Liu, S., … Xu, W. (2018). Emerging function and potential diagnostic value of circular RNAs in cancer. *Molecular Cancer*, *17*(1), 123.

Dragomir, M., & Calin, G. A. (2018). Circular RNAs in cancer - lessons learned from microRNAs. *Frontiers in Oncology*, *8*, 307.

Eckert, A. W., Kappler, M., Schubert, J., & Taubert, H. (2012). Correlation of expression of hypoxia-related proteins with prognosis in oral squamous cell carcinoma patients. *Oral and Maxillofacial Surgery*, *16*, 189–196.

Evan, G., & Littlewood, T. (1998). A matter of life and cell death. *Science*, *281*(5381), 1317–1322.

Feller, L., & Lemmer, J. (2012). Oral squamous cell carcinoma: Epidemiology, clinical presentation and treatment. *J Cancer Ther*, *3*, 263–268.

Greene, J., Baird, A. M., Brady, L., Lim, M., Gray, S. G., McDermott, R., & Finn, S. P. (2017). Circular RNAs: Biogenesis, function and role in human diseases. *Frontiers in Molecular Biosciences*, *4*, 38.

Haddad, R. I., & Shin, D. M. (2008). Recent advances in head and neck cancer. *New England Journal of Medicine*, *359*, 1143–1154.

Hansen, T. B., Jensen, T. I., Clausen, B. H., Bramsen, J. B., Finsen, B., Damgaard, C. K., & Kjems, J. (2013). Natural RNA circles function as efficient microRNA sponges. *Nature*, *495*(7441), 384–388.

Heo, K., Kim, Y. H., Sung, H. J., Li, H. Y., Yoo, C. W., Kim, J. Y., … Choi, S. W. (2012). Hypoxia-induced upregulation of apelin is associated with a poor prognosis in oral squamous cell carcinoma patients. *Oral Oncology*, *48*, 500–506.

Jeck, W. R., Sorrentino, J. A., Wang, K., Slevin, M. K., Burd, C. E., Liu, J., … Sharpless, N. E. (2013). Circular RNAs are abundant, conserved, and associated with ALU repeats. *RNA*, *19*, 141–157.

Jirawatnotai, S., Hu, Y., Livingston, D. M., & Sicinski, P. (2012). Proteomic identification of a direct role for Cyclin D1 in DNA damage repair. *Cancer Research*, *72*, 4289–4293.

Kristensen, L. S., Hansen, T. B., Venø, M. T., & Kjems, J. (2018). Circular RNAs in cancer: Opportunities and challenges in the field. *Oncogene*, *37*(5), 555–565.

Li, Z., Huang, C., Bao, C., Chen, L., Lin, M., Wang, X., … Shan, G. (2015). Exon-intron circular RNAs regulate transcription in the nucleus. *Nature Structural & Molecular Biology*, *22*, 256–264.

Memczak, S., Jens, M., Elefsinioti, A., Torti, F., Krueger, J., Rybak, A., … Rajewsky, N. (2013). Circular RNAs are a large class of animal RNAs with regulatory potency. *Nature*, *495*, 333–338.

Noguti, J., De Moura, C. F., De Jesus, G. P., Da Silva, V. H., Hossaka, T. A., Oshima, C. T., & Ribeiro, D. A. (2012). Metastasis from oral cancer: An overview. *Cancer Genomics & Proteomics*, *9*, 329–335.

Ocana, A., Vera-Badillo, F., Al-Mubarak, M., Templeton, A. J., Corrales-Sanchez, V., Diez-Gonzalez, L., … Amir, E. (2014). Activation of the PI3K/mTOR/AKT pathway and survival in solid tumors: Systematic review and meta-analysis. *PLoS One*, *9*(4), e95219.

Panda, A. C., De, S., Grammatikakis, I., Munk, R., Yang, X., Piao, Y., … Gorospe, M. (2017). High-purity circular RNA isolation method (RPAD) reveals vast collection of intronic circRNAs. *Nucleic Acids Research*, *45*, e116–e116.

Parkin, D. M., Bray, F., Ferlay, J., & Pisani, P. (2001). Estimating the world cancer burden: Globocan 2000. *International Journal of Cancer*, *94*, 153–156.

Patop, I. L., & Kadener, S. (2018). CircRNAs in Cancer. *Current Opinion in Genetics & Development*, *48*, 121–127.

Rehan, M., & Bajouh, O. S. (2019). Virtual screening of naphthoquinone analogs for potent inhibitors against the cancer signaling PI3K/AKT/mTOR pathway. *Journal of Cellular Biochemistry*, *120*(2), 1328-1339.

Rivas, S., Gómez-Oro, C., Antón, I., & Wandosell, F. (2018). Role of Akt isoforms controlling cancer stem cell survival, phenotype and self-renewal. *Biomedicines*, *6*(1), 29.

Salzman, J., Gawad, C., Wang, P. L., Lacayo, N., & Brown, P. O. (2012). Circular RNAs are the predominant transcript isoform from hundreds of human genes in diverse cell types. *PLoS One*, *7*, e30733.

Siegel, R. L., Miller, K. D., & Jemal, A. (2016). Cancer statistics, 2016. *CA: A Cancer Journal for Clinicians*, *66*, 7e30–30e30.

Suzuki, H., & Tsukahara, T. (2014). A view of pre-mRNA splicing from RNase R resistant RNAs. *International Journal of Molecular Sciences*, *15*, 9331–9342.

Thompson, L. (2006). World Health Organization classification of tumours: pathology and genetics of head and neck tumours. *Ear Nose Throat J*, *85*(2), 74.

Van Dijk, B. A. C., Brands, M. T., Geurts, S. M. E., Merkx, M. A. W., & Roodenburg, J. L. N. (2016). Trends in oral cavity cancer incidence, mortality, survival and treatment in The Netherlands. *International Journal of Cancer*, *139*, 574e83–583e83.

Vokes, E. E., Weichselbaum, R. R., Lippman, S. M., & Hong, W. K. (1993). Head and neck cancer. *New England Journal of Medicine*, *328*, 184–194.

Wang, Y. -F., Li, B. -W., Sun, S., Li, X., Su, W., Wang, Z. -H., … Yang, H. -Y. (2018). Circular RNA expression in oral squamous cell carcinoma. *Frontiers in Oncology*, *8*, 398.

World Health Organization classification of tumors: Pathology and genetics of head and neck tumors. (2016). *Ear, Nose, and Throat Journal*, *85*(2), 74.

Xu, X., Zhou, L., Yu, C., Shen, B., Feng, J., & Yu, S. (2018). Advances of circular RNAs in carcinoma. *Biomedicine & Pharmacotherapy = Biomédecine & Pharmacothérapie*, *107*, 59–71.

Zbaren, P., & Lehmann, W. (1987). Frequency and sites of distant metastases in head and neck squamous cell carcinoma. *Archives of Otolaryngology–Head and Neck Surgery*, *113*, 762–764.

SUPPORTING INFORMATION

Additional supporting information may be found online in the Supporting Information section at the end of the article.

How to cite this article: Wen S, Yufan W, Feng W, Biru Z, Hanyu Z, Hongyu Y. Circular RNA hsa_circ_0007059 indicates prognosis and influences malignant behavior via AKT/mTOR in oral squamous cell carcinoma. *J Cell Physiol*. 2019;234: 15156–15166. https://doi.org/10.1002/jcp.28156